J Nanopart Res (2023) 25:103
https://doi.org/10.1007/s11051-023-05755-w

RESEARCH PAPER

Rapid template-assisted self-assembly: a practical route to the fast assembly of colloidal particles

Ayoub Laghrissi · Prince Gupta · Horst-Günter Rubahn · Jacek Fiutowski

Received: 5 January 2023 / Accepted: 27 April 2023 / Published online: 10 May 2023

Abstract Simple and quick techniques for assembling nanoparticles in topographically designed Poly(dimethylsiloxane) moulds of nanosized shapes have great potential in many spectroscopic and sensing tools. Close-packed particles pose rich plasmonic resonances, enabling the optical response to be tailored on both the nano- and macroscale. Template-assisted self-assembly (TASA) is a method that creates colloidal aggregates with controlled sizes formed by dewetting aqueous dispersions of NPs across surfaces. We present rapid TASA (rTASA), a modified version with an overall process time of under 10 min, improving speed and user-friendliness. Depending on the array pitch distance and average number of NPs per trap, the transmission through the template drops by between 20 and 80%, enabling them to be detected with even the simplest spectroscopic solutions. This rapid method is useful as a building block to generate self-assembled systems that exhibit exciting optical properties in crucial areas, particularly in building a fast test for size-selective NP detection.

A. Laghrissi (✉) · P. Gupta · H.-G. Rubahn · J. Fiutowski (✉)
Mads Clausen Institute, NanoSYD, University of Southern Denmark, Alsion 2, 6400 Sønderborg, Denmark
e-mail: laghrissi@mci.sdu.dk

J. Fiutowski
e-mail: fiutowski@mci.sdu.dk

Keywords Colloidal particles · CAPA · TASA · rTASA · Assembly · SERS · 2-Naphthalenethiol · Optical properties

Introduction

Many scientific fields and technologies involve nanosized objects, structures, and materials. Nanoparticles (NPs) formed the core of the nanotechnology revolution of the last century and have proven applications in many fields, such as electronics, aerospace, energy, and medicine [1–4]. The increasing demand for products containing NPs and the constant discovery of new functions that leverage their beneficial effects are accompanied by a potential risk that limits the usability of nanoengineered particles in medicine, cosmetics, and the food industry. In particular, NPs below a critical size brings general concerns since it was shown that they could overcome natural cell barriers and cause cytotoxic effect [5–8]. In recent years, extensive research has demonstrated that NPs' size, shape, and chemical composition are the main factors influencing their toxicity [5–8]. Testing the NPs, with a special focus on their size, becomes a crucial step in risk assessment to follow the rapid commercialisation of nano-enabled products and ensure safe and sustainable nanomaterials use.

Consequently, there is an urgent need to develop appropriate, cost-effective assessment and prediction methods. The assessment method should provide

the best decision criteria to determine whether a product is safe or needs better NPs control. Such a method could provide researchers, manufacturers and regulators with a risk assessment tool that considers essential specifications like speed, simplicity, and flexibility. Currently, the main approaches to risk assessment depend on the type of sample preparation. One direction is to prepare a sample in liquid form without processing; in this case, the size and concentration of specific NPs are tested and determined without removing them from the solution by using optical methods such as dynamic light scattering (DLS) [9–11]. Another approach requires fixation for modern microscopy, where the NPs must be collected before removal from the solution. This approach includes the drop-casting and/or alignment of the NPs [12, 13], with various aggregation dynamics [14, 15]

Li et al. [16] have summarised various assembly methods and discussed the mechanisms behind self-assembly and triggered assembly in standard methods. Template-assisted self-assembly (TASA) offers reasonable simplicity compared to procedures that alter the surface of NPs to enable assembly. A glass cover encloses colloidal particles in prefabricated traps so that their self-assembly occurs locally [16, 17]. The glass cover later serves as the receiving substrate onto which the assemblies are stamped. Capillary-assisted particle assembly (CAPA) [18–21] is another promising, highly efficient, versatile and scalable method. It exploits the extensive capillary interactions in a colloidal suspension. By bringing a droplet of suspension into contact with a structured surface, the localisation and organisation of the particles can be controlled in predefined patterns. Both methods have proven valuable for the alignment of NPs. TASA incorporates NPs onto a receiving substrate through the use of a template. The template supports the nanoparticles, allowing them to attain their desired shape before being imprinted onto the receiving substrate. This differs from CAPA, which utilises capillary forces to organise NPs into selected traps.

This manuscript reports a new method, Rapid Template-Assisted Self-Assembly (rTASA), a unique combination of simplicity and speed, with an assembly time of just 10 min, enabling assembly NPs in traps and making them ready for further analysis or usage. In contrast to other methods requiring high-precision equipment, rTASA needs only consumable-based elastomeric replicas, making it an accessible and cost-effective technique. Notably, compared to the CAPA method, the rTASA method could lead to more accurate and faster detection of NPs while minimising the required control parameters (i.e. temperature, meniscus velocity and contact angle). This process results in a highly precise and accurate incorporation of NPs, ultimately enhancing the substrate's properties and functionality, highlighting its novelty and potential for various applications. rTASA can be used with simple optical methods, e.g. a drop in light transmission of 20–80%, depending on the average number of NPs, paving the way for efficient detection and size-selective recognition of NPs. Additionally, we proved the usability for SERS, providing signal enhancement of sulphur-containing species on silver nanoparticles.

Materials and methods

Elastomer replicas with well-defined circular arrays were used in all subsequent experiments. Electron beam lithography (EBL) produced a silicon template replicating structured PDMS [13]. A thin layer of poly (methyl methacrylate) (PMMA, MicroChem) was spin-coated onto a silicon substrate, and then a total area of (3 × 1 mm) was subjected to EBL. Si/PMMA was then immersed in a mixture of isopropyl alcohol (Technic France) and methyl isobutyl ketone (MicroChem) 4:1 for 45 s for development, then rinsed well with isopropyl alcohol. After that, 200 nm of titanium was deposited on the Si/PMMA using electron beam evaporation using a PVD device (Cryofox 600) and dipped in remover PG (MicroChem) to remove the PMMA and Ti-layer, leaving only the Ti pillars. A non-stick coating of trichloro-(1H,1H,2H,2H-perfluorooctyl) silane (Sigma Aldrich) was applied to the Si template. Surface silanization was carried out in a special vacuum chamber at a pressure of 10 mbar for 10 min, followed by drying on a hot plate at 120 °C for 10 min. The PDMS (Sylgard 184) and curing agent were mixed in a 10:1 ratio and degassed to remove oxygen bubbles. The mixture was dropped onto the silicon master moulds and dried at 120 °C for 40 min to produce the PDMS image to entrap the NPs.

The microstructure and morphology of the NPs were characterised using a high-resolution scanning

electron microscope (SEM, Hitachi S-4800). The SEM also has an electron beam lithography package (RAITH GmbH).

For surface-enhanced Raman spectroscopy (SERS) measurements, a 10^{-3} M aqueous solution of 2-Naphthalenethiol (NPT, TermoFischer) was prepared in ethanol to the required concentration. The substrate was cleaned of residues using a 1:2 hydrochloric acid (Sigma Aldrich) and ethanol mixture. Samples were soaked in a 10^{-3} M concentrated solution for 1 h. After drying, the excess of non-bound molecules was removed using ethanol. Raman measurements were performed on a confocal Raman microscope (alpha300 WITec) using a 532-nm laser beam and a laser power of 0.1 mW. The integration time was 10 s. The Raman signal was recorded using a CCD camera. A 50 nm ag layer on unstructured and structured PDMS was used as a reference.

Results and discussion

Rapid templates-assisted self-assembly

The conventional TASA method for assembling densely packed clusters has already been described in detail [16, 17]. A colloidal NPs dispersion is dropped onto a structured surface (e.g. a PDMS surface). A hydrophilic cover glass is placed on the PDMS surface to disperse the droplet with the NPs. It traps them to self-arrange and controls the evaporation and re-deposition to overcome the biggest drop-casting challenge related to the coffee ring effect (CRE), first observed by Deegan et al. [21, 22]. The degree of hydrophilicity of the glass slide decides whether the NPs remain in the traps or are stamped onto the glass slide, which serves as the receiving substrate. After 1–2 h, the colloidal dispersion dries, and the glass slide is carefully removed, carrying the well-assembled NPs.

Here, we present a variation of TASA that achieves comparable results but is far less complex. The main aim is to accelerate the process by bringing the NPs into the PDMS traps by dropping them directly on the patterned surface without the glass slide agent. The biggest challenge when drop-casting a dispersion of NPs onto the substrate is CRE, first observed by Deegan et al. [20, 21]. The liquid flows from the drop's centre to the edge during evaporation. The NPs accumulate at the edges, similar to the ring-shaped spot left by a coffee drop on a smooth surface after drying. Depending on the contact angle of the liquid surface, there are two possible states — Cassie–Baxter and Wenzel — with the latter being relevant for PDMS moulds [23]. When a liquid comes into contact with a structured surface (e.g. PDMS), the liquid completely wets the surface. In other words, the contact area between liquid and solid is maximised and obeys the Wenzel equation:

$$cos(\theta_w) = r.cos(\theta) \tag{1}$$

which states that $\theta_W < \theta$ when the CA $\theta < 90°$. Therefore, rough surfaces trap the fluid in the holes, making them immobile. This reduces the fluid flow responsible for the coffee ring effect so that the NPs are evenly distributed on the surface after completely evaporating (Fig. 1).

The self-assembly properties of NPs depend on numerous fundamental factors, including interactions between NPs, surface tension and externally supported approaches. Interactions such as the van der Waals interaction and the Colombian interaction, together with forces emanating from the PDMS surface and external factors such as evaporation, are the main driving forces in droplet casting [24, 25]. As mentioned earlier, the trapping of the NPs is triggered by the disturbance of the particles on the PDMS surface to ensure that they are held in the trap and do not migrate to the side of the droplet on the PDMS. The geometry of the template determines the retention forces. For a microdroplet of NP on the PDMS surface (regardless of geometry), the forces exerted on each NP can be expressed as follows:

$$F_{tot,i} = F_{ad} + F_{vdW} + F_c + F_{fl} \tag{2}$$

F_c and F_{vdW} are the Colombian and van der Waals interactions between the NPs and represent the residual attractive or repulsive forces, which are considered to be among the fundamental mechanisms causing the self-assembly of individual NPs into different nanostructures. A fad is the adhesion force between the particle and the substrate and is only slightly affected by changing the geometry of the PDMS, as it depends on the distance between the NP and the

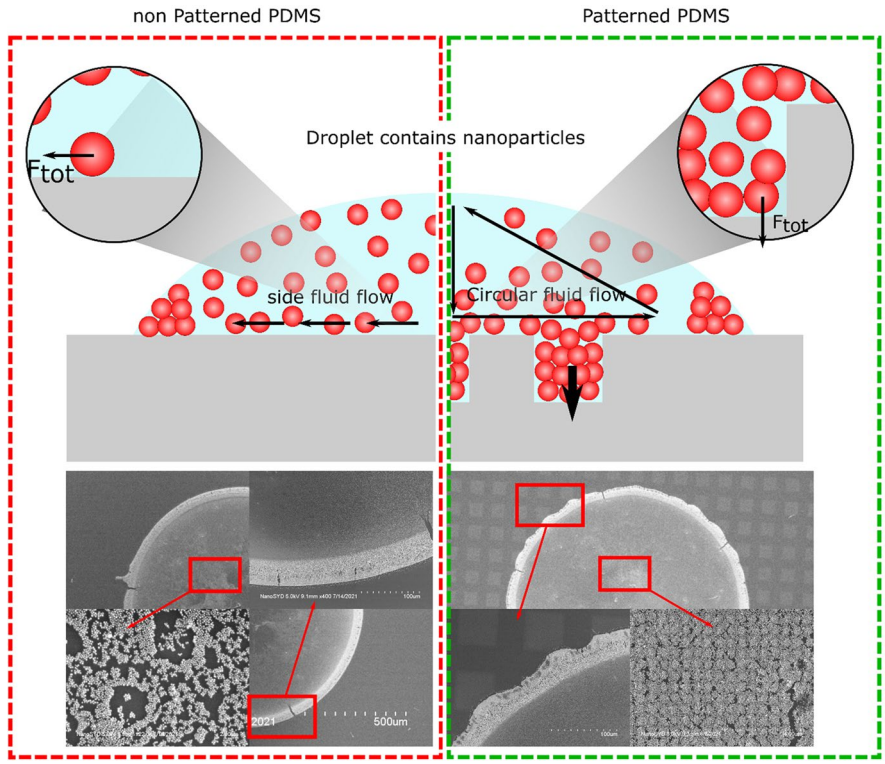

Fig. 1 Illustrative representation of the mechanisms of NPs deposition on the unstructured PDMS surface (left) and the structured PDMS surface (right)

surface. The flow force F_{fl} is the key that controls the motion and pinning of the NPs. A radially outward capillary flow from the centre towards the contact line is observed, driven by evaporation, as evaporation is strongest at the edge, which is more 'aerated' than the centre of the droplet, causing the lateral flow of NPs. However, nano/microstructures on the surface would exert capillary-trapping forces and the outward capillary flow. The two compete and change the flow from lateral to circular, resulting in less mobility of the trapped NPs.

$$F_{fl} = \begin{cases} F_{c,evap} & no\ traps \\ F_{c,evap} + F_{c,trap} & traps \end{cases} \quad (3)$$

A dispersion of a 5-µl mixture of 3.10^{10} particles/ml Ag (Nanocomposix), DMF (Sigma Aldrich) and ethanol (1:1:3) was dropped onto the unstructured and structured PDMS surface (Fig. 1) under ambient temperature and air atmosphere; ethanol was used owing to its high wettability and ability to facilitate evaporation. The droplet volume and ethanol content in the dispersion determines the time required for the dispersion to evaporate. However, it is short, not exceeding 10 min at room temperature. Figure 1 shows the non-patterned PDMS surface where the coffee ring effect occurs. The NPs form a ring-like pattern on the PDMS surface, depositing firmly at the edges. Their concentration gradually decreases towards the centre of the dried droplet, and they do not show any pattern or uniformity. Using a patterned PDMS surface reduces the coffee ring effect but does not eliminate it; a ring of concentrated NPs is still present (although less than non-patterned PDMS). Unfortunately, a quantitative assessment of the NP concentration in the edge region is impossible, but it is visible in the Scanning Electron Microscope (SEM) image. The crucial area to examine is the centre of the droplet, where the holes are located. Figure 1 shows the NP distribution over the holes. A complete filling of the holes with NPs can be observed, and the NPs appear densely packed. This contrasts with what is observed in the space between the holes, where the NPs are present in a lower concentration than in the holes. The difference in the distribution of the NPs in the holes and on the sides does not contradict the Wenzel condition; the holes help keep the liquid together with the NPs. Another observation favouring

the NPs and attachment is that the outer shape of the coffee ring has a wavy profile, and the NPs are attached to the holes that are not completely covered by the droplet.

The method of rTASA is shown in Fig. 2. The starting point is a patterned PDMS surface with circular traps corresponding to the intended sizes of the trapped NPs (Fig. 2a). Then, a droplet containing an NPs dispersion is applied to the surface of the PDMS shape (Fig. 2b). At this point, the droplet is usually covered with a glass slide (TASA) to transport the particles onto the glass slide. The rTASA bypasses this step, allowing the droplet to dry rapidly and trap the NPs in the PDMS holes. When chemicals such as ethanol are dried, light and a heat source are used to shorten the drying time. The NPs remaining on the traps' edges or the flat PDMS surface (Fig. 2c) are removed in the subsequent cleaning step (Fig. 2d), where a 'sticky' surface can be placed in contact with the PDMS top and lifted off with the excess NPs, leaving the trapped NPs not altered. This cleaning step can be done several times to achieve the desired effect (Fig. 2e). Once the cleaning is complete, the NPs will be well-packed in the PDMS traps and ready for further characterisation.

Following the rTASA process described, a 1:3 Ag:EtOH mixture was dropped onto the PDMS surface. After completion of the drying step, the traps were filled (Fig. 3a), yet the NPs were still sitting on the PDMS surface. Here the additional cleaning step removes the excess NPs from the surface. A 'sticky' surface is used to remove the excess NPs. Adhesive tape could be a destructive cleaning tool, removing the NPs from the traps and leaving polymeric adhesive on them, potentially changing their properties. Therefore, the cleaning approach involves hydrating a plasma-cleaned glass slide with a mixture of water and ethanol. Hydrating the slide improves its adhesive properties in a controlled manner so that only the excess is removed from the surface. Figure 3b shows that, after the surface is cleaned, the traps are filled with densely packed NPs, and no excess remains. The coffee ring effect is less significant in rTASA, where the NPs are dropped onto patterned PDMS. The patterns on the PDMS surface enable the Wenzel condition, which results in the pinning of the NPs, and the additional cleaning step guarantees exclusive deposition of the NPs in the traps. The process is rapid; desiccants such as ethanol as a heat source and light could further speed up the drying step.

A test was run to compare the novel process described in this letter with another particle assembly method CAPA. Although highly precise, CAPA is among the most complex and time-consuming methods due to the numerous control parameters. The overall CAPA process is well described elsewhere [18–20]. The following experimental parameters were used in CAPA. A mixture of 50 nm Ag-NPs:ethanol:DMF (1:4:1) was sandwiched between PDMS and a glass slide. The glass slide started moving at a constant rate of 1 mm/s at 35 °C to create an accumulation zone and the correct evaporation rate. As the meniscus moves, the NPs obey a laminar flow and make their way to the accumulation zone, where the concentration of NPs is highest. At this moment and during evaporation, the NPs jump into the holes, remain behind the meniscus' capillary forces and become trapped in the holes. Scanning electron micrographs (Fig. 3c) show deposited Ag-NPs in PDMS holes aiming at close packing of the NPs. Therefore, the deposition parameters were chosen accordingly, including the height and concentration in the accumulation zone.

The microscopic images show the long-range ordering of the close-packed filling of the holes. Looking back at the results of the rTASA method

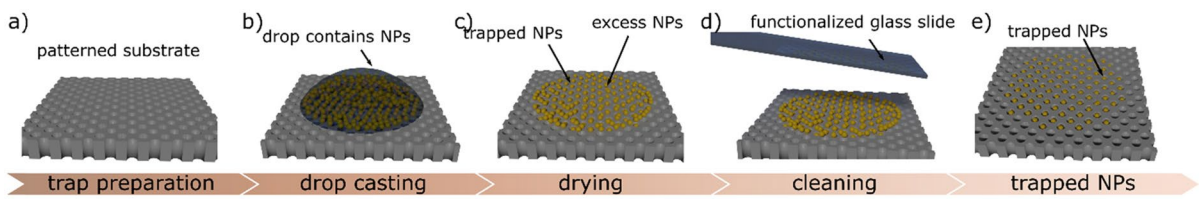

Fig. 2 Schematic representation of rTASA: **a** patterned PDMS, **b** drop casting of aqueous NP dispersion onto the surface of patterned PDMS, **c** the drying process, **d** cleaning the excess NPs from the PDMS surface, and **e** the traps containing the composite NPs

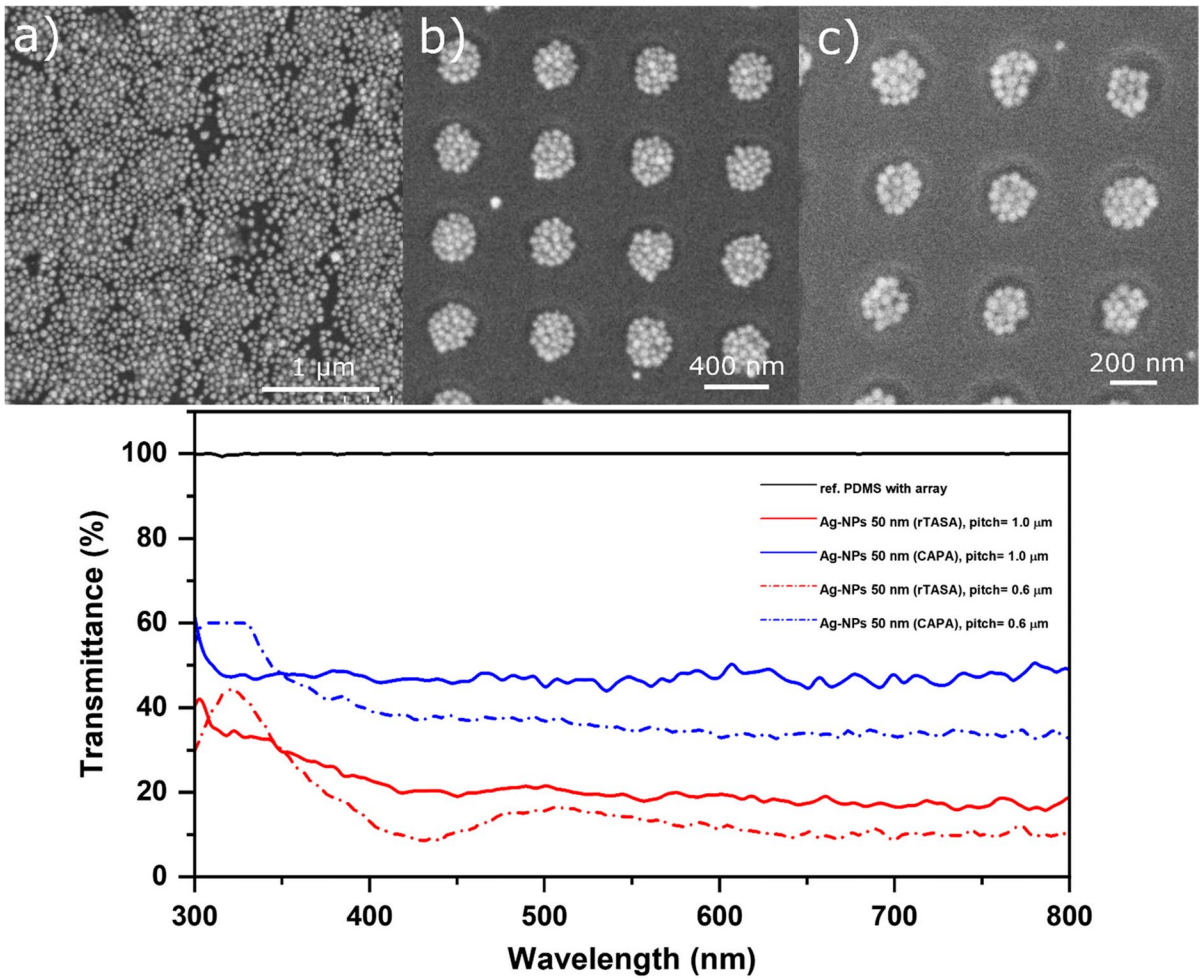

Fig. 3 Upper panel: representative SEM images of **a** the PDMS surface after drop-casting the NPs, **b** the deposited NPs with rTASA, and **c** the deposited NPs with CAPA. Bottom panel: measured optical transmittance for different deposition methods (CAPA and rTASA) at different trap spacings

reveals similarities between the methods in dense packing, high filling and long-range ordering. There are only two differences. The first concerns the degree of complexity of the methods, as CAPA proves to be more complex than rTASA. Second, in CAPA the deposition of certain NP sizes is determined not only by trap size but also by trap depth, which means that larger particles are less likely to settle on the traps but may still do so, questioning the size selectivity of the method. The additional cleaning step to remove excess NP in rTASA ensures that only particles smaller than the trap size are captured because the trap size is the threshold size of the NPs.

Optical properties

The optical properties of the trapped NPs were further assessed by the light transmission drop they caused compared to the empty traps. Figure 3d shows the transmission in a 300–800-nm wavelength range using a low-precision spectrometer. We found that the trapped NPs cause a decrease in transmission compared to the empty PDMS. Apart from the minor differences in the transmittance drop between rTASA and CAPA, the sensitivity of the rTASA method is comparable to that of CAPA. To increase the technique's sensitivity in NPs detection, smaller pitches

were investigated, which showed a sharp drop in light transmission. Small pitches can condense the particle pocket and improve detection when the NP concentration is low. We present particle detection and risk assessment as application examples. Still, the method has a wide field of application, especially concerning plasmonic (lattice resonances, super crystal arrays, etc.) and material detection and/or custom surface-enhanced Raman spectroscopy (substrate formation, custom self-assembly, plasmonic metasurface, etc.).

Surface-enhanced Raman scattering

Surface-enhanced Raman spectroscopy (SERS) is an effective analytical technique to study the properties of molecules on the surface of Ag NPs. By utilising the strong electromagnetic field derived from the plasmonic property of Ag, chemical compounds bound to the surface of NPs can be detected. The Raman scattering from molecules that interact with the surface of Ag-NPs is greatly amplified, making it possible to identify molecules at extremely low concentrations. Many surface molecules, including proteins, DNA, lipids, and tiny molecules, have been studied using this method. SERS has also been used to investigate the surface chemistry of NPs and find compounds in the nanomolar range. SERS has given researchers new insights into the structure and operation of molecules on the surface of NPs by harnessing the plasmonic characteristics of Ag-NPs. The adsorption of sulphur-containing species with a concentration of thiols on the NP surface can further improve the SERS of Ag-NPs. Thiols interact with Ag-NPs to produce powerful chemisorption interactions that can improve the attached molecules' Raman scattering.

Figure 4 shows Raman spectra of NPT measured on different substrates together with the empirical approach to SERS EF obtained using Eq. 4.

$$EF = \left(\frac{I_{SERS}}{C_{SERS}} \frac{C_{RS}}{I_{RS}} \right) \tag{4}$$

where I_{SERS} Is the Raman-band intensity corresponding to the concentration C_{SERS} of the substance analysed on the SERS Substrate, and I_{RS} and C_{RS} The intensity and concentration on the non-SERS substrate, respectively.

Compared with the spectrum obtained for NPT, an overall improved signal was received for NPT on all the tested samples. Structured Ag films, consisting of a 50-nm Ag layer evaporated onto PDMS surfaces with nanoscale elements (traps), have significantly enhanced the Raman signal compared to planar Ag films (50 nm). This enhancement is due to the increased surface area and charge transfer between the metal surface and the analyte molecules. The increased surface area allows more analyte molecules to interact with the metal surface, increasing Raman scattering events. In addition, the nanoscale features of the Ag surface create hot spots with an increased electric field, which facilitates charge transfer of analyte molecules. This charge transfer further amplifies the Raman signal by increasing the molecule's population of electronically excited states.

The 50 nm and 100 nm have been found to have significantly higher surface-enhanced Raman scattering (SERS) than the structured and unstructured Ag films. The trapped Ag-NPs 50 nm had the highest Raman enhancement with an enhancement factor of up to 10^4. The 100-nm Ag-NPs show lower enhancement. This increase can be attributed to increased surface enhancement due to the larger surface area of the small-size NPs. As a result, Trapped Ag NPs are advantageous for SERS applications due to their large surface area and enhanced charge transfer. These results provide insight into the size-dependent Raman enhancement of Ag-NPs of sulphur-containing species, which can be used to improve the sensitivity and selectivity of SERS for sensing and detection applications. However, it is not our goal to highlight the results obtained in this work as opposed to those obtained elsewhere but to emphasise the crucial role of the rTASA method in easily arranging NPs for different applications.

Conclusions

In summary, we presented rTASA, a new method for nanoparticle assembly based on the drop-casting dispersion of nanoparticles in droplet form on collecting traps. The results allow for comparison to high-precision methods, like CAPA, however, being more cost- and time-effective. In addition, using desiccants such as ethanol as a heat and light source, the entire process could speed it up further. The rTASA has been proven to be an efficient method for preparing tailored arrays of NPs in traps, where the subsequent cleaning

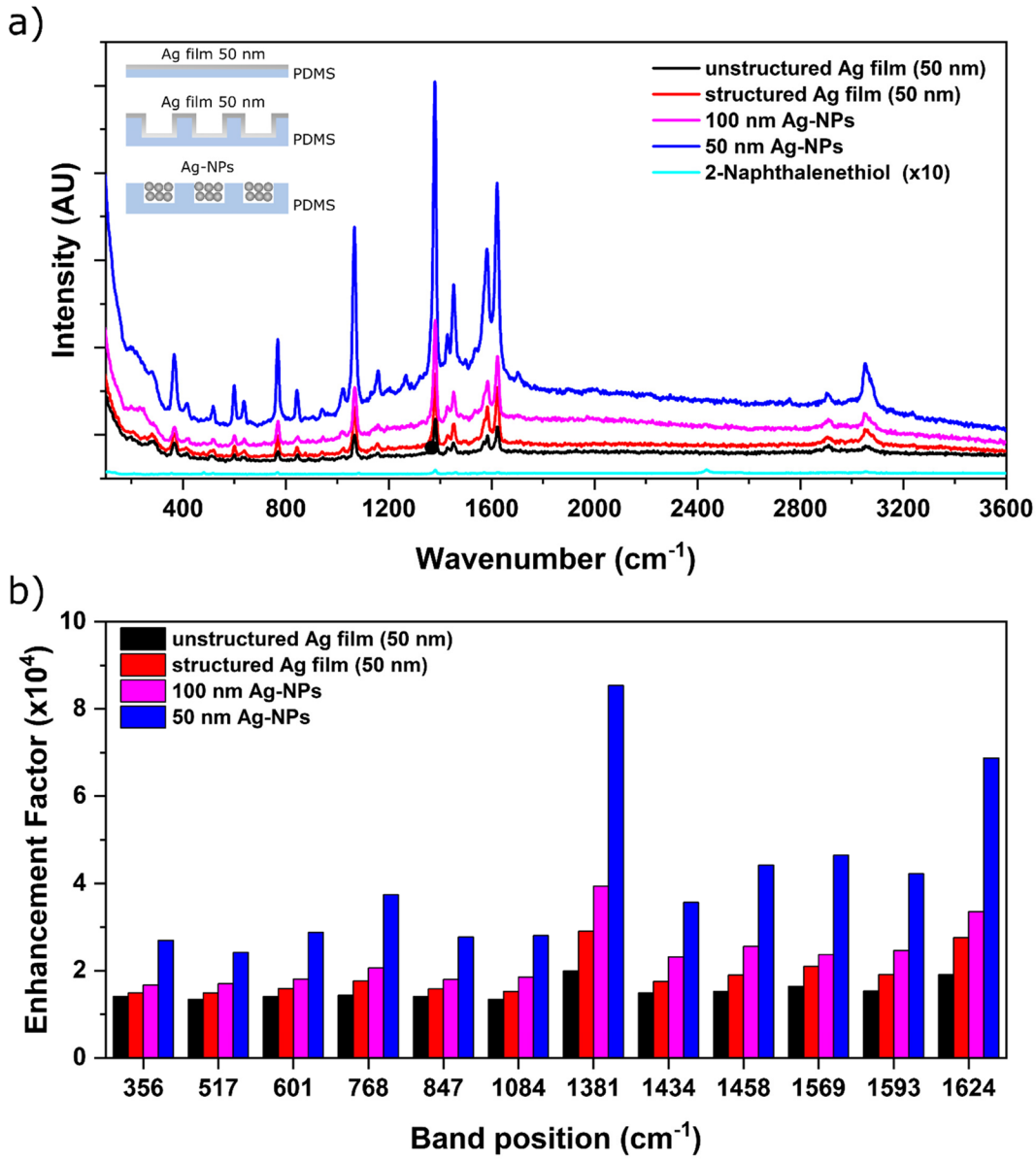

Fig. 4 **a** Raman scattering spectra of NPT on non-SERS and SERS substrates. **b** SERS enhancement factor (EF) for different NPT bands

step is crucial for size-selective trapping. In turn, the size selectivity depends only on the size of traps, which could allow single or more dense NPs arrangements. The entrapped NPs cause a drop in light transmission, enabling far-field nanoparticle detection.

We have limited our discussion to Ag-NPs; however, the technique can be applied to other particle classes besides metallic particles, e.g. polymers and microplastics. We have already successfully implemented the method for polystyrene, magnetic iron oxide and polymer-coated gold nanoparticles [26]. This effort led to the development of programmable nanoparticle-based devices. Hence the rTASA opens the door for future applications like nano-based drug delivery or general sensing and detection, including preparing SERS substrates.

Acknowledgements We are grateful to the European Regional Development Fund Interreg Deutschland-Danmark under project number 086-1.1-17 (CheckNano), the Villum Foundation, the Experiment program, and the project NanoTrain (REF. 00035903) for financial support. Many thanks to Dr Mindaugas Juodėnas and Dr Tomas Tamulevičius for their help in the CAPA setup. And PhD student Nadzeya Khinevich for her input on SERS measurements.

Funding Open access funding provided by Royal Danish Library

Data availability Data, associated metadata, and calculation tools are available from the corresponding authors.

Declarations

Conflict of interest The authors have no known competing financial or other interests in the present study.

References

1. Chaudhery MH (2018) Handbook of nanomaterials for industrial applications. Elsevier. https://doi.org/10.1016/C2016-0-04427-3
2. Khan ZH (2018) Nanomaterials and their applications. Springer, Singapore. https://doi.org/10.1007/978-981-10-6214-8
3. Cai Z, Li F, Rong M, Lin L, Yao Q, Huang Y, Chen X, Wang X (2019) Novel nanomaterials for biomedical, environmental and energy applications. Elsevier, ISBN, p 9780128144978
4. Pradeep T (2009) Noble metal nanoparticles for water purification: a critical review. Thin Solid Films 517:6441–6478
5. Barua S, Mitragotri S (2014) Challenges associated with penetration of nanoparticles across cell and tissue barriers: a review of current status and future prospects. Nano Today 9:223–243. https://doi.org/10.1016/j.nantod.2014.04.008
6. Hainan S, Cuijuan J, Ling W, Xue B, Shumei Z (2019) Cytotoxicity-related bioeffects induced by nanoparticles: the role of surface chemistry. Front Bioeng Biotechnol 7:414. https://doi.org/10.3389/fbioe.2019.00414
7. Zhang B, Sai Lung P, Zhao S, Chu Z, Chrzanowski W, Li Q (2017) Shape-dependent cytotoxicity of PLGA-PEG nanoparticles on human cells. Sci Rep 7:7315. https://doi.org/10.1038/s41598-017-07588-9
8. Lewinski N, Colvin V, Drezek R (2018) Cytotoxicity of nanoparticles. Small 4:26–49. https://doi.org/10.1002/smll.200700595
9. Dahneke BE (1983) Measurement of suspended particles by quasielastic light scattering. J Polym Sci Polym Lett Ed 21:570
10. Pecora R (1985) Dynamic light scattering: applications of photon correlation spectroscopy. Plenum Press. https://doi.org/10.1007/978-1-4613-2389-1
11. Stetefeld J, McKenna SA, Patel TR (2016) Dynamic light scattering: a practical guide and applications in biomedical sciences. Biophys Rev 8:409–427. https://doi.org/10.1007/s12551-016-0218-6
12. Kumar AKS, Zhang Y, Li D, Compton RG (2020) A mini-review: how reliable is the drop casting technique? Electrochem Commun 121:106867. https://doi.org/10.1016/j.elecom.2020.106867
13. Chen CY, Chang CH, Wang CM, Li YJ, Chu HY, Chan HH, Huang YW, Liao WS (2018) Large area nanoparticle alignment by chemical lift-off lithography. Nanomaterials 8:71. https://doi.org/10.3390/nano8020071
14. Abdellatif MH, Abdelrasoul GN, Scarpellini A, Marras S, Diaspro A (2015) Induced growth of dendrite gold nanostructure by controlling self-assembly aggregation dynamics. J Colloid Interface Sci 458:266–272. https://doi.org/10.1016/j.jcis.2015.07.055
15. Abdellatif MH, Abdelrasoul GN, Salerno M, Liakos I, Scarpellini A, Marras S, Diaspro A (2016) Fractal analysis of inter-particle interaction forces in gold nanoparticle aggregates. Colloids Surf, A 497:225–232. https://doi.org/10.1016/j.colsurfa.2016.03.013
16. Li Z, Fan Q, Yin Y (2022) Colloidal self-assembly approaches to smart nanostructured materials. Chem Rev 122:4976–5067. https://doi.org/10.1021/acs.chemrev.1c00482
17. Scarabelli L, Vila-Liarte D, Mihi A, Liz-Marzán LM (2021) Templated colloidal self-assembly for lattice plasmon engineering. Accounts Mater Res 2:816–827. https://doi.org/10.1021/accountsmr.1c00106
18. Chen J, Guo L, Qiu B, Lin Z, Wang T (2018) Application of ordered nanoparticle self-assemblies in surface-enhanced spectroscopy. Mater Chem Front 5:835–860. https://doi.org/10.1039/C7QM00557A
19. Ni S, Lucio I, Heiko W (2018) Capillary assembly as a tool for the heterogeneous integration of micro- and nanoscale objects. Soft Matter 16:2978–2995. https://doi.org/10.1039/C7SM02496G
20. Virganavičius D, Juodėnas M, Tamulevičius T, Schift H, Tamulevičius S (2017) Investigation of transient dynamics of capillary assisted particle assembly yield. App Surf Sci 406:136–143. https://doi.org/10.1016/j.apsusc.2017.02.100
21. Deegan RD, Bakajin O, Dupont TF, Huber G, Nagel SR, Witten TA (1997) Capillary flow as the cause of ring stains from dried liquid drops. Nature 389:827–829. https://doi.org/10.1038/s41586-021-03444-z

22. Deegan RD (2000) Pattern formation in drying drops. Phys Rev E 61:475. https://doi.org/10.1103/PhysRevE.61.475
23 Ko HY, Park J, Shin H, Moon J (2004) Rapid self-assembly of monodisperse colloidal spheres in an ink-jet printed droplet. Chem Mater 16:4212–4215. https://doi.org/10.1021/cm035256t
24. Behrens SH, Borkovec M, Schurtenberger P (1998) Aggregation in charge-stabilized colloidal suspensions revisited. Langmuir 14:1951–1954. https://doi.org/10.1021/la971237k
25. Grasso D, Subramaniam K, Butkus M, Strevett K, Bergendahl J (2002) A review of non-DLVO interactions in environmental colloidal systems. Rev Environ Sci Biotechnol 1:17–38. https://doi.org/10.1023/A:1015146710500
26. Laghrissi A, Rubahn HG, Fiutowski J (2023) Nano-based drug delivery system using magnetic and PNIPAm coated gold nanoparticles. Manuscript in preparation